

Origin of bulklike optical response in noble-metal Ag and Au nanoparticlesJ. C. Idrobo^{1,2} and S. T. Pantelides^{1,2}¹*Department of Physics and Astronomy, Vanderbilt University, Nashville, Tennessee 37235, USA*²*Materials Science and Technology Division, Oak Ridge National Laboratory, P.O. Box 2008, Oak Ridge, Tennessee 37831, USA*

(Received 22 January 2010; revised manuscript received 14 April 2010; published 12 August 2010)

The origin of bulklike optical response of noble (silver and gold) metal nanoparticles has been studied using classical (Mie) and time-dependent density-functional theories. We find that the bulklike optical response in the noble-metal nanoparticles is determined more strongly by the electronic d character of the valence electrons than the atomic coordination or size of the nanoparticles. The importance of Coulomb and exchange-correlation interactions to model optical responses is also discussed.

DOI: [10.1103/PhysRevB.82.085420](https://doi.org/10.1103/PhysRevB.82.085420)

PACS number(s): 73.22.-f, 78.67.Bf, 71.45.Gm, 71.15.Mb

I. INTRODUCTION

Noble nanoparticles (gold and silver) are well known to alter the visual appearance of dielectric host materials when their size, shape, and spatial distribution are modified.^{1,2} This physical phenomenon can easily be described using theories based on classical electrodynamics when the particles are several nanometers in diameter.³ But as the nanoparticle size decreases, quantum effects become more important and classical theories become insufficient to describe optical excitations. It was recently reported that the optical absorption of some Ag nanoparticles formed by as few as ten atoms in vacuum could be modeled by phenomenological classical (Mie) theory.⁴ In contrast, a similar theoretical study of the optical properties of Au nanoparticles, of equivalent size as the Ag nanoparticles, shows that Au nanoparticles have intrinsic quantumlike optical behavior that cannot be captured by classical theories.^{5,6} It can be argued that the difference in the optical response between silver and gold nanoparticles arises from intrinsic differences in their atomic and electronic structures. The obvious question is then, what are those intrinsic differences that allow only some Ag atomic-scale particles to show a classical-like optical response? Similarly, why Au nanoparticles do not present a classical-like optical response at the same size regime as the Ag nanoparticles?

In this paper, we investigate the origin of the bulklike optical response of noble (silver and gold) metal nanoparticles in vacuum using classical (Mie) and time-dependent density-functional theories (TDDFTs). We calculate the absorption spectra of particles with fcc and non-fcc (lowest-energy isomers in vacuum) bonding configuration. The particles are composed between 12 and 55 atoms and their diameter ranges from 0.8 to 1.2 nm. We find that the bulklike optical response of Ag and Au nanoparticles is strongly correlated with the d -like character of the valence electrons, i.e., the larger the electronic d character the stronger the bulklike optical response. We find that atomic coordination and particle size are less important than the d character of the valence electrons in determining the bulklike optical response of the Ag and Au nanoparticles. We also investigated the role of Coulomb and exchange-correlation interactions in the nanoparticles' optical excitations within time-dependent density-functional theory. We find that in the absence of

Coulomb interactions, the absorption spectra of the Au and Ag nanoparticles shift a few electron volts to lower energies, while their oscillator strengths get enhanced. When exchange-correlation interactions are not taken into account, the absorption spectra shift slightly (fractions of electron volts) to higher optical excitations while the oscillator strengths decrease only moderately. These results show how the intrinsic quantum properties of noble-metal nanoparticles become dominant in optical excitations as particle size decreases.

We start by discussing the differences and similarities of the absorption spectra of Ag and Au nanoparticles of two previous theoretical studies.^{4,6} Figure 1 shows the atomic structure and the absorption spectra of Ag₁₂ and Au₅₀. Both, Ag₁₂ and Au₅₀ do not have bulklike fcc structures. All their atoms are either undercoordinated or overcoordinated. The absorption spectra of the Ag₁₂ and Au₅₀ nanoparticles were calculated using first-principles calculations within TD local-density approximation (TDLDA) and classical (Mie) theories. The details of those two theoretical methods will be discussed shortly. It can clearly be seen in Fig. 1(a) that the quantum and classical predictions of the Ag₁₂ absorption spectra (in particular, the energy and intensity of the main plasmon peak ~ 3.5 eV) agree extraordinarily well between each other and with the experimental measurement. In the case of the Au₅₀ nanoparticle, there exists no experimental data. However, it can clearly be seen [Fig. 1(b)] that the Mie and TDLDA predictions differ drastically from each other. While the classical absorption spectrum shows a Mie plasmon peak at ~ 2.4 eV the absorption spectrum calculated within TDLDA shows only a monotonic increase in the oscillator strength as a function of energy. It is probable that the different optical properties of Ag and Au nanoparticles could arise from their shape, size, or/and intrinsic electronic properties. Therefore, in order to understand how particle size and shape, atomic and electronic configuration affect the optical response of silver and gold nanoparticles, we have performed the following set of calculations. First, we selected atomic-scale particle sizes that are comparable with those of the Ag₁₂ and Au₅₀ nanoparticles but with a fcc bonding configuration. Figure 2 shows the atomic structure of the two nanoparticles studied (either 13 atoms of Ag/Au for the smaller particles and 55 Ag/Au atoms for the larger particles, respectively). Then, we calculated their optical spectra using the TDLDA and Mie theories.

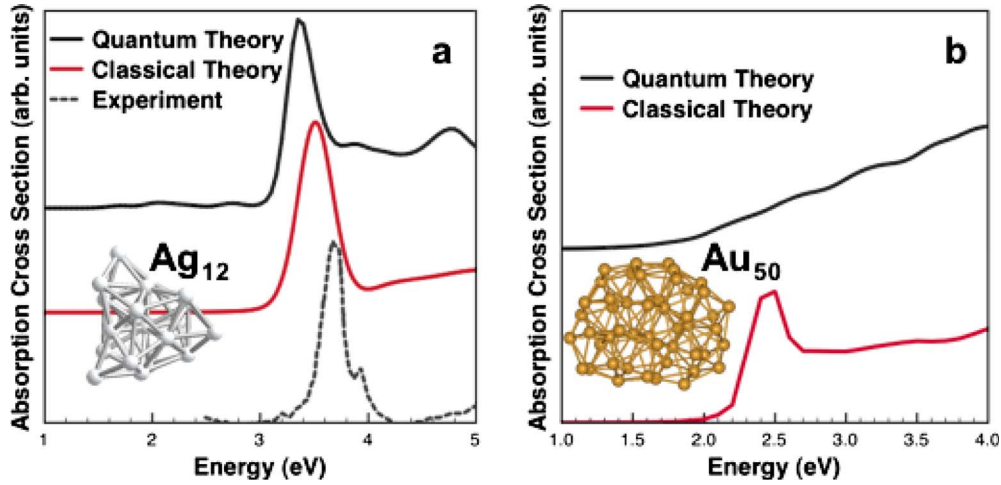


FIG. 1. (Color online) Theoretical (classical-Mie- and quantum-TDLDA-) and experimental optical spectra of Ag_{12} and Au_{50} nanoparticles. Both nanoparticles are the calculated lowest energy structures in vacuum. The diameter of Ag_{12} and Au_{50} is 0.8 nm and 1.2 nm, respectively. Data obtained from Refs. 4 and 6.

II. METHODS

A. Quantum theory

In order to obtain the optical response of the Ag and Au nanoparticles within a first-principles approach, we solved the Kohn-Sham equations of the nanoparticles in real space within the framework of the higher-order finite-difference *ab initio* pseudopotential method,⁸ and utilizing a Chebyshev-Davidson eigenvalue algorithm.⁹ A three-dimensional Cartesian grid with a uniform spacing was used, and the nanoparticles were placed in a large spherical domain, outside of which their wave functions were required to vanish. We employed scalar-relativistic Troullier-Martins pseudopotentials¹⁰ in nonlocal form¹¹ generated from the reference configurations $4d^{10}5s^{15}p^0$ and $5d^{10}6s^{16}p^0$ for silver and gold, respectively. The optical-absorption spectra of the nanoparticles were calculated using a linear-response formalism within TDDFT.^{12,13} In this formalism, and in the limit of a very weak external potential, the system (nanoparticle) responds only through the dynamical polarizability, $\alpha(\omega)$, which is defined as

$$\alpha(\omega) = \sum_n \frac{f_n}{\Omega_n^2 - \omega^2}. \quad (1)$$

Ω_n are the optical excitation energies of the system and f_n are the oscillator strengths. Following Casida's notation for unpolarized spin systems,¹² Ω_n 's are calculated by diagonalizing the full interaction matrix which includes all collective excitations,

$$(\omega_{ij}^2 \delta_{ik,jl} + 2\sqrt{\lambda_{ij}\omega_{ij}} K_{ij,kl} \sqrt{\lambda_{kl}\omega_{kl}}) F_n = \Omega_n^2 F_n, \quad (2)$$

where (i,k) and (j,l) refer to Kohn-Sham occupied and unoccupied states, respectively. $\omega_{ij} = \epsilon_j - \epsilon_i$ and $\lambda_{ij} = n_j - n_i$ are the differences of the eigenvalues and the occupation numbers, respectively. The oscillator strengths f_n are calculated from the eigenvectors F_n with the following relationship:

$$f_n = \frac{2}{3} \sum_{\beta=\{x,y,z\}} |\hat{\beta}(\delta_{i,k}\delta_{j,l}\lambda_{kl}\omega_{kl})^{1/2} F_n|^2, \quad (3)$$

where $\hat{\beta}$ is a unit vector pointing in any of the three orthogonal Cartesian coordinates. $K_{ij,kl}$ is the coupling kernel that describes the screening of the electromagnetic field by the system. It is defined by

$$K_{ij,kl} = \int \int \phi_i^* \phi_j \left(\frac{e^2}{|\mathbf{r} - \mathbf{r}'|} + f_{xc} \right) \phi_k \phi_l^* d\mathbf{r} d\mathbf{r}'. \quad (4)$$

The first term on the right-hand side of Eq. (4) is the electrostatic screening produced by electrons and holes interacting via a Coulomb mechanism (K_C) while the second term is the screening produced by electrons and holes interacting through quantum-mechanical exchange and correlation (K_{xc}). In the random-phase approximation, the exchange and correlation is ignored and set to zero. In TDDFT, the exchange and correlation kernel is a functional derivative of the exchange-correlation potential, $f_{xc} = \delta V_{xc} / \delta \rho$. Within TDLDA, f_{xc} becomes local and energy independent. Both the ground-state Kohn-Sham wave functions and the absorption spectra were calculated using the PARSEC code.⁸ The important parameters that control the convergence of the optical

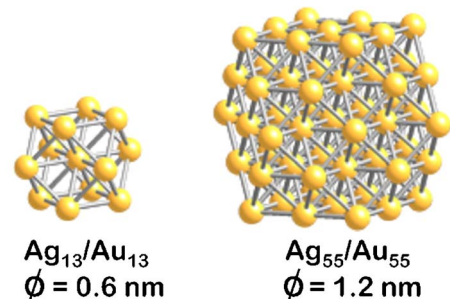


FIG. 2. (Color online) Atomic structure of silver and gold nanoparticles with a fcc bonding configuration.

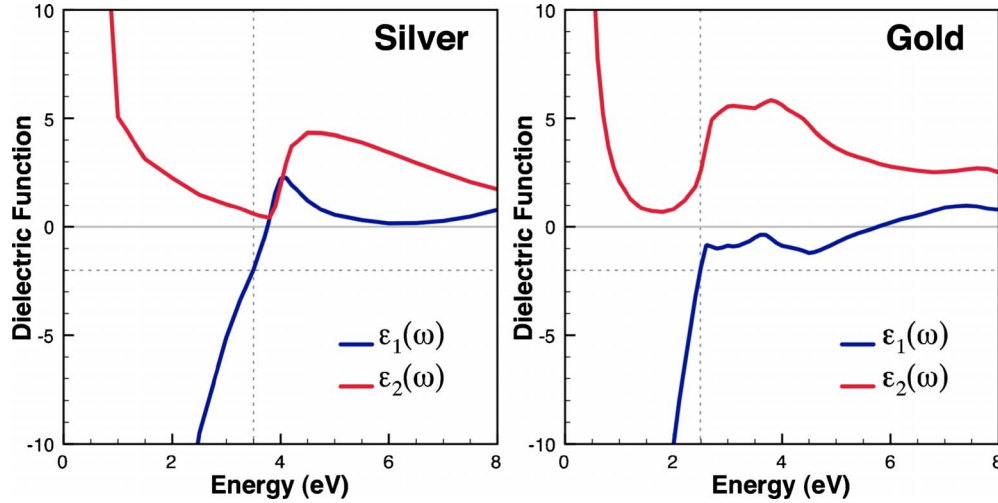


FIG. 3. (Color online) Real $\epsilon_1(\omega)$ and imaginary $\epsilon_2(\omega)$ part of the dielectric function of bulk silver and gold bulk (fcc). The dashed lines highlight the $\epsilon_1(\omega)$ value when the Mie resonance peak condition is satisfied in vacuum. Experimental data obtained from Ref. 7.

spectra and, consequently, the extent of the memory and computational requirements are the grid spacing h , the radius of the sphere R_{max} , and the total number of the valence-conduction Kohn-Sham pairs, N_{vc} . N_{vc} determines the final size of the interaction TDLDA matrix. In the present calculations, we used a grid size $h=0.4$ a.u. and $R_{max}=30$ a.u., which gives a total number of grid points of $\sim 1\,760\,000$ that later were reduced to $\sim 220\,000$ due to symmetry operations. The size of the TDLDA matrices ranged from $\sim 16\,000$ to $\sim 90\,000$ for the Ag_{13}/Au_{13} and Ag_{55}/Au_{55} nanoparticles, respectively. The above choice of parameters allowed us to obtain absorption spectra converged up to 6 eV. The suitability of TDLDA to calculate optical spectra of nanoparticles has been validated repeatedly for many different species (Na, Si, Ag, and Au).^{4,5,13–16}

B. Classical theory

To calculate the optical spectra within classical methods, we used Mie theory, which was developed by Gustav Mie in the early 1900s to explain the absorption and scattering of small metallic particles embedded in dielectric media.¹ Mie theory consists in solving Maxwell's equations for electromagnetic plane waves interacting with metallic particles that are smaller than the wavelength, λ , of light (dipole approximation). The solution to that problem is a complicated series expansion in powers of R/λ , (where R is the particle radius). The first term of that expansion is the absorption cross section, which is given by

$$\sigma_{abs}(\omega) = \frac{9\omega V}{c} \frac{\epsilon_2(\omega)}{[\epsilon_1(\omega) + 2]^2 + \epsilon_2(\omega)^2}, \quad (5)$$

when the dielectric medium is vacuum. $\epsilon_1(\omega)$ and $\epsilon_2(\omega)$ are the real and imaginary parts of the dielectric function of the constituent material (silver or gold), c is the speed of light, and V is the volume of the nanoparticles. The contribution of higher-order R/λ terms in Eq. (5) are negligible for particles of ~ 1 nm in diameter and therefore are not taken into account in this study, i.e., the smallest R/λ ratio in the energy

range of the calculated absorption spectra (1–5 eV or a λ of 1240–248 nm, respectively) is $R/\lambda=1/248=0.004$. The resonance condition in vacuum (Mie or plasmon peak) occurs when $\epsilon_1(\omega)=-2$ and $\epsilon_2(\omega)$ is small. The Mie condition is reached at $\omega \sim 3.2$ eV and $\omega \sim 2.4$ eV for bulk silver and bulk gold, respectively, as it is shown in Fig. 3.

III. RESULTS

Figure 4 shows the optical response of four particles (Ag_{13} , Ag_{55} , Au_{13} , and Au_{55}) obtained by TDLDA and Mie theories. The optical response obtained using Mie theory for both fcc-structure Ag nanoparticles is in reasonably good agreement with the TDLDA calculations, indicating an intrinsic bulklike optical response of the Ag nanoparticles. More specifically, the TDLDA spectra of the fcc-structure Ag nanoparticles exhibit a peak at the same energy (3.2 eV) as the plasmon (Mie) peak predicted by Mie theory. The agreement between both theoretical predictions is better for Ag_{55} than Ag_{13} , indicating that particle size plays a stronger role in controlling the optical excitations of the smaller particle. We also noticed that among the three Ag nanoparticles (Ag_{12} , Ag_{13} , and Ag_{55}), the optical response of the non-fcc Ag_{12} (which has a similar particle size than Ag_{13}) nanoparticle is the one that has the strongest intrinsic bulklike optical behavior.

In the case of the Au nanoparticles, only the TDLDA optical response of the Au_{55} nanoparticle exhibits features that are similar to what is expected for a nanoparticle with a bulklike optical response. In particular, the fcc Au_{55} TDLDA spectrum has a Mie peak but it is shifted to higher energies by 0.8 eV with respect to the classical prediction (2.4 eV). While for the smaller Au nanoparticle (Au_{13}), the TDLDA spectrum has two peaks and therefore cannot be associated with the gold Mie peak. Since we find that particles of the same size, shape, and bonding configuration but with different constituent material, (i.e., Ag_{55} vs Au_{55}) have a different optical response, we proceeded to investigate the role of electronic interactions in controlling the optical excitations

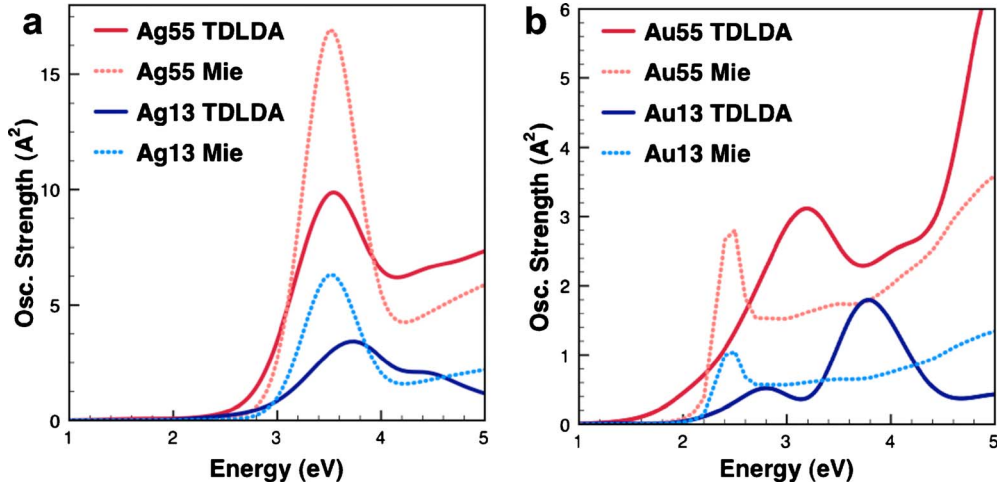


FIG. 4. (Color online) Calculated optical spectra of fcc-like bonded (a) Ag₁₃, Ag₅₅ and (b) Au₁₃, Au₅₅ nanoparticles using classical (Mie) and quantum (TDLDA) theories.

of the Ag and Au nanoparticles. As it was mentioned earlier, within the TDLDA formalism, there are only two interactions (or kernels) that contribute to the optical response of the nanoparticles, Coulomb interaction (K_C), and exchange and correlation interaction (K_{xc}). Thus, we proceeded to calculate again the optical response of all the nanoparticles (fcc-like structures and the non-fcc structures) but by explicitly switching off the K_C and the K_{xc} kernels in the interaction matrix shown in Eq. (1). Figure 5 shows the optical response of Ag₅₅ and Au₅₅ calculated with both K_C and K_{xc} kernels and with only one of the kernels. As it is shown in Fig. 5, as soon as K_C is switched off the Mie peaks of the Ag₅₅ and Au₅₅ nanoparticles are strongly shifted to lower energies and their intensity overestimated. Electronic exchange and correlation only shifts slightly (tenths of electron volts) the spectra to higher energies for both nanoparticles. We find the same kind of behavior for the rest of the nanoparticles. The small contribution of the K_{xc} kernel to the optical response of the noble-metal nanoparticles indicates that the bulklike optical

response in the Ag and Au nanoparticles is mainly arising from an electronic Coulomb-type interaction. However, after all the analysis just mentioned, we still do not know the reason why some nanoparticles have an intrinsic bulklike optical response and some not.

To address how electronic interactions control the optical response of the gold and silver nanoparticles, we have projected the ground energy spectrum of all the nanoparticles according to their electronic s , p , or d character. Then we mapped the states that contribute explicitly to the optical excitations that form the Mie peak using the method described in Ref. 15, which is given by the following formula:

$$\%Elec_{s,p,d} = \frac{\sum_n f_n \sum_{vc} |F_n^{vc}|^2 |\langle \Psi_{s,p,d} | \phi_v \rangle|^2}{\sum_n f_n}, \quad (6)$$

where f_n are the oscillator strengths and the coefficients $|F_n^{vc}|$

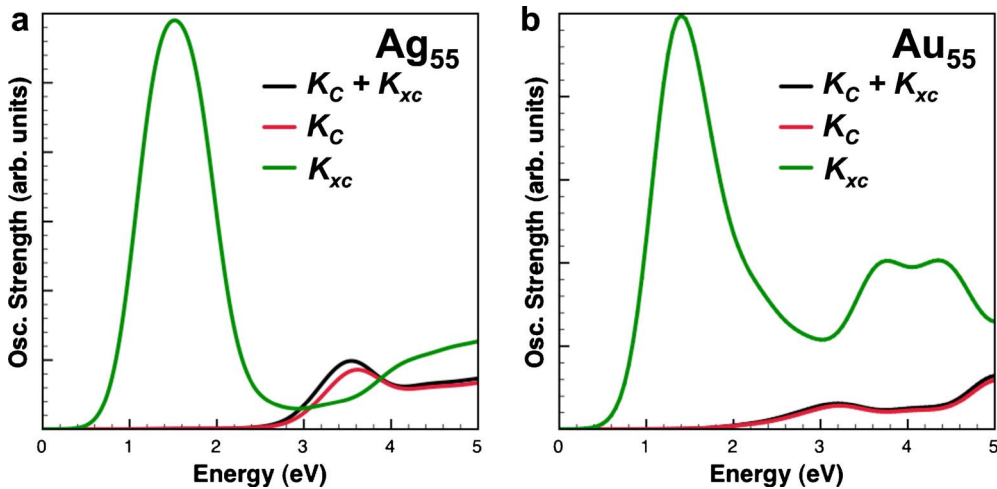


FIG. 5. (Color online) Optical response of the fcc-like bonded (a) Ag₅₅ and (b) Au₅₅ nanoparticles when both Coulomb (K_C) and exchange and correlation (K_{xc}) kernels are used in the TDLDA formalism (black line) compared with the optical response obtained when only K_C (red line) or K_{xc} (green line) kernel are used to calculate the optical spectra.

Ground State Energy Spectrum

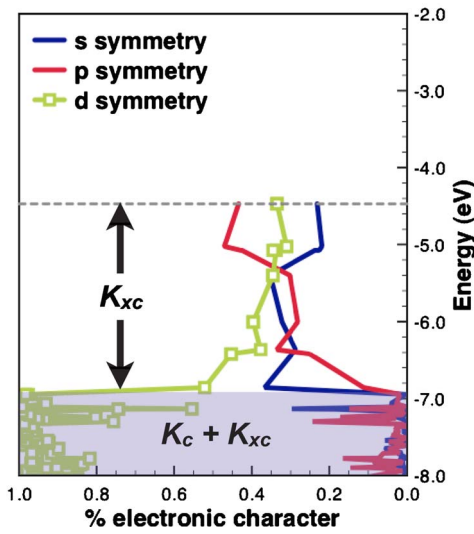


FIG. 6. (Color online) Ground-state energy spectrum of the fcc Ag_{55} nanoparticle decomposed accordingly with its electronic s , p , and d characters. The shaded (purple) area highlights the states that contribute the most (81%) to the Mie peak, i.e., when both kernels K_C and K_{xc} are calculated [solid black line in Fig. 5(a)] while the black arrow highlights the states that contribute (99%) to the Mie peak when only K_{xc} is calculated [solid green line in Fig. 5(a)]. The dotted line indicates the energy value of the highest-occupied molecular orbital.

are the weight factors of the valence-conduction vc orbital pairs contributing to the optical excitations Ω_n . $\langle \Psi_{s,p,d} | \phi_v \rangle$ are either the s , p , or d projection of the valence orbitals ϕ_v . The sum in n includes all the optical excitations that form the Mie peak. The electronic character mapping of the optical

excitations was done for the cases when the optical spectra were calculated with both K_C and K_{xc} kernels and with only one of the kernels at the time. Figure 6 shows the ground-state energy spectrum of the fcc Ag_{55} nanoparticle when the K_C and K_{xc} kernels and when only K_{xc} are used to calculate the optical spectra. It can be observed in Fig. 6 that when both electronic interactions, K_C and K_{xc} , are present in the optical spectra, 81% of the valence states that contribute to the Mie peak have a strong d character. But when the Coulomb interaction is turned off, 99% of the states that contribute the Mie peak have a really low d character. We also observed the same general behavior for the other Ag and Au nanoparticles. However, the d character present in the Mie peak is smaller for both fcc Ag_{13} and Au_{13} nanoparticles than that of their larger counterparts, Au_{55} and Au_{50} nanoparticles. In other words, the increase in d contribution in the optical spectra results in a screening of the s electrons and consequently a reduction in the oscillator strengths. Similar behavior in the optical spectra of Ag_n , $n=1-8$ clusters has also been reported.¹⁵

A more interesting correlation arises when we compare the states contributing to the Mie peak, their electronic character, and the optical spectra between nanoparticles. For instance, Fig. 7 shows the ground-state energy spectrum and contribution to the Mie peak of fcc Au_{55} and non-fcc Au_{50} nanoparticles. It can be clearly seen that 84% of the states that contribute to the Mie peak for the fcc Au_{55} nanoparticle have a strong d character and even several of those states reach a 100% d character. In contrast, for the non-fcc Au_{50} nanoparticle, only 46% of the states that contribute to the optical excitations, in the energy range where the Mie peak should be present ~ 2.4 eV, have a large d character, and none of them actually reach a 100% d character. Analyzing the electronic character of the ground-state energy spectrum of the non-fcc Au_{50} nanoparticle it can be understood why its

Ground State Energy Spectrum

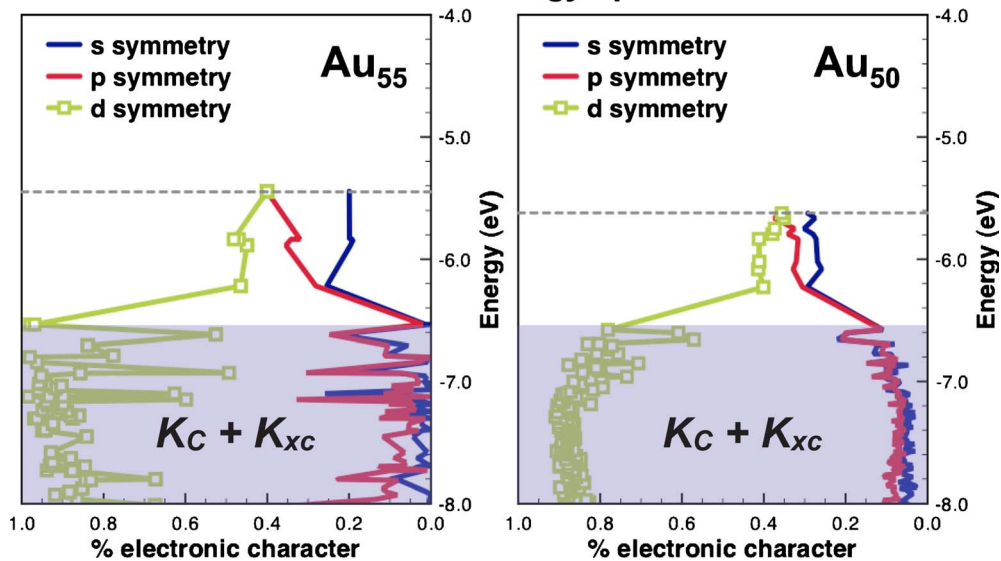


FIG. 7. (Color online) Ground-state energy spectrum of the Au_{55} and Au_{50} nanoparticles decomposed accordingly with its electronic s , p , and d characters. The shaded (purple) area highlights the states that contribute the most (84% and 46%, for Au_{55} and Au_{50} , respectively) to the Mie peak, i.e., when both kernels K_C and K_{xc} are calculated. The dotted line indicates the energy value of the highest-occupied molecular orbital.

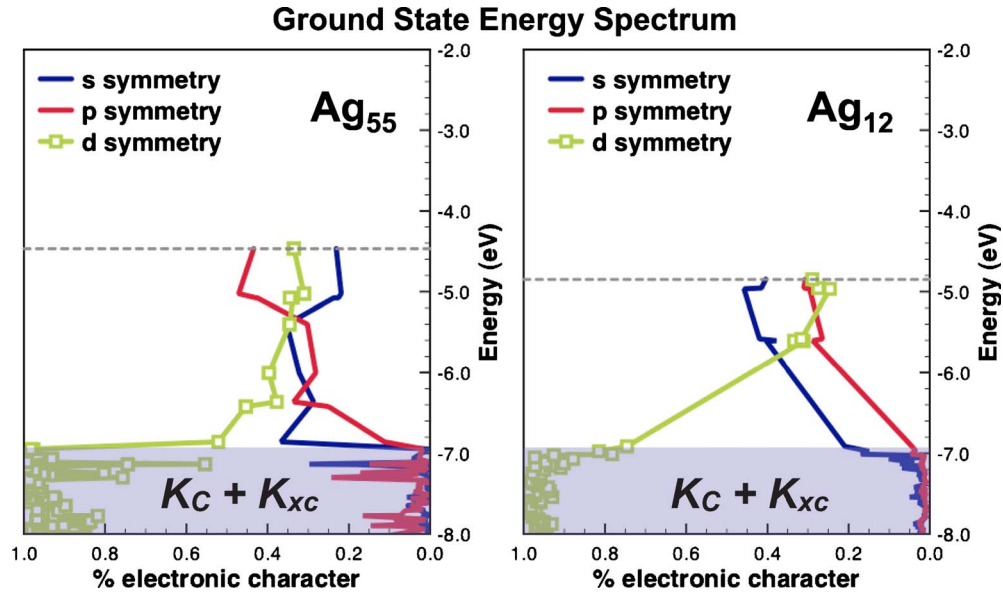


FIG. 8. (Color online) Ground-state energy spectrum of the Ag_{55} and Ag_{12} nanoparticles decomposed accordingly with its electronic s , p , and d characters. The shaded (purple) area highlights the states that contribute the most (81% and 35%, for Ag_{55} and Ag_{12} , respectively) to the Mie peak, i.e., when both kernels K_C and K_{XC} are calculated. The dotted line indicates the energy value of the highest-occupied molecular orbital.

optical spectrum [Fig. 1(b)] does not present a Mie peak. The total overall d character of the states that contribute to the optical excitations below ~ 3 eV in the non-fcc Au_{50} nanoparticle is really small.

Figure 8 shows the ground-state energy spectrum and contribution to the Mie peak of fcc Ag_{55} and non-fcc Ag_{12} nanoparticles. For the Ag_{55} nanoparticle 81% of the states that contribute to the Mie peak have a large d character while for the Ag_{12} nanoparticle that value only reaches 35%. However, the great majority of the Ag_{12} states contributing to the Mie peak have a d character close to 100% while for the Ag_{55} states the d character varies in a range between 55%

and 100%. We also calculated the percent electronic character for bulk fcc Ag and Au within density-functional theory using the projector augmented wave method¹⁷ as it is shown in Fig. 9. Using Fig. 9 as a reference, it can clearly be seen that the electronic character of all the Ag and Au nanoparticles resembles those of Ag and Au bulk, respectively. However, the nanoparticles that present the stronger bulklike optical responses are the ones that have their electronic d character closer to that of their respective bulk, independently of their size or bonding configuration. That is the case for the non-fcc Ag_{12} nanoparticle when compared with respect to the other nanoparticles of this study.

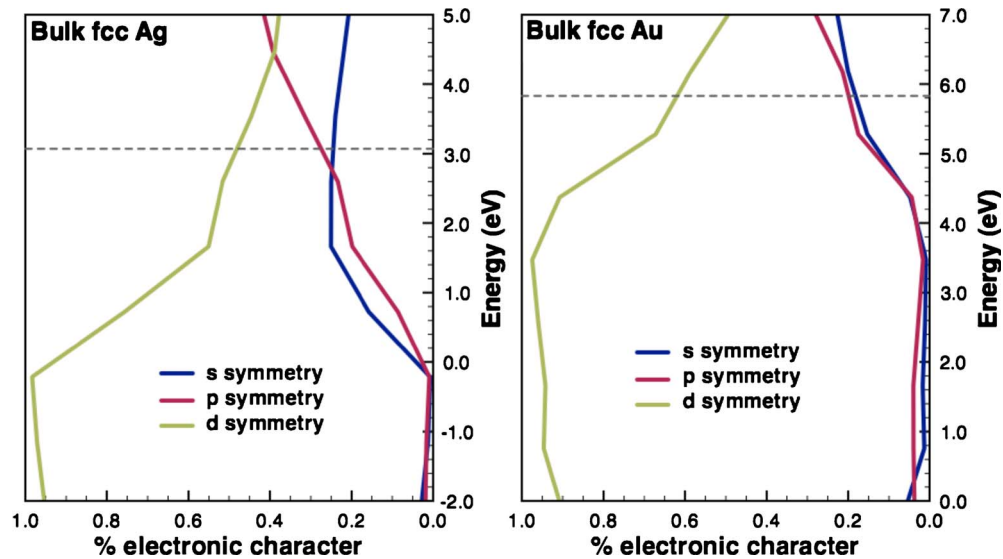


FIG. 9. (Color online) Ground-state energy spectrum of bulk fcc Ag and Au decomposed accordingly with its electronic s , p , and d characters. The dotted line indicates the value for the Fermi energy.

IV. SUMMARY

In summary, our theoretical calculations show that in order for noble-metal nanoparticles to present an intrinsic bulklike optical response in their absorption spectra, the optical electronic interaction at low energies has to be mainly dominated by valence states with a strong electronic d character. We find that as long as that condition is satisfied, atomic coordination, particle size, and shape become secondary in contributing to a bulklike optical response for Ag and Au nanoparticles smaller than 1.2 nm. We have also investigated the role of Coulomb and exchange-correlation interactions in the optical excitations within time-dependent density-functional theory. We find that Coulomb interactions control the optical excitation energy and oscillator strengths in the absorption spectra of the Au and Ag nanoparticles. Exchange and correlation interactions are less important in the optical excitations. We find that the absence of exchange and corre-

lation in the TDLDA interaction matrix shifts slightly (fractions of electron volts) the spectra to higher optical excitations and also decreases the oscillator strengths moderately. The present results show how the intrinsic quantum properties of noble-metal nanoparticles become dominant in optical excitations as particle size decreases.

ACKNOWLEDGMENTS

This work was supported in part by the National Science Foundation GOALI under Grant No. DMR-0513048, by Alcoa, Inc., by the McMinn Endowment at Vanderbilt University, and by the Division of Materials Sciences and Engineering, U.S. Department of Energy under contract with UT-Battelle. This research used resources of the National Energy Research Scientific Computing Center, which is supported by the Office of Science of the U.S. Department of Energy under Contract No. DE-AC02-05CH11231.

-
- ¹G. Mie, *Ann. Phys.* **330**, 377 (1908).
²R. Gans, *Ann. Phys.* **342**, 881 (1912).
³H. C. Van de Hulst, *Light Scattering by Small Particles* (Wiley, New York, 1957).
⁴K. Baishya, J. C. Idrobo, S. Ögüt, M. Yang, K. Jackson, and J. Jellinek, *Phys. Rev. B* **78**, 075439 (2008).
⁵J. C. Idrobo, W. Walkosz, S. F. Yip, S. Ögüt, J. Wang, and J. Jellinek, *Phys. Rev. B* **76**, 205422 (2007).
⁶J. C. Idrobo, S. Ögüt, M. Yang, K. Jackson, and J. Jellinek, (unpublished).
⁷*CRC Handbook of Chemistry and Physics*, 87th ed., edited by D. R. Lide, (Taylor & Francis, Boca Raton, FL, 2007).
⁸J. R. Chelikowsky, N. Troullier, and Y. Saad, *Phys. Rev. Lett.* **72**, 1240 (1994); J. R. Chelikowsky, N. Troullier, K. Wu, and Y. Saad, *Phys. Rev. B* **50**, 11355 (1994).
⁹Y. Zhou, Y. Saad, M. L. Tiago, and J. R. Chelikowsky, *Phys. Rev. E* **74**, 066704 (2006).
¹⁰N. Troullier and J. L. Martins, *Phys. Rev. B* **43**, 1993 (1991).
¹¹L. Kleinman and D. M. Bylander, *Phys. Rev. Lett.* **48**, 1425 (1982).
¹²M. E. Casida, in *Recent Advances in Density-Functional Methods, Part I*, edited by D. P. Chong (World Scientific, Singapore, 1995), p. 155; in *Recent Developments and Applications of Modern Density Functional Theory*, edited by J. M. Seminario (Elsevier, Amsterdam, 1996), p. 391.
¹³I. Vasiliev, S. Ögüt, and J. R. Chelikowsky, *Phys. Rev. B* **65**, 115416 (2002).
¹⁴M. L. Tiago, J. C. Idrobo, S. Ögüt, J. Jellinek, and J. R. Chelikowsky, *Phys. Rev. B* **79**, 155419 (2009).
¹⁵J. C. Idrobo, S. Ögüt, and J. Jellinek, *Phys. Rev. B* **72**, 085445 (2005).
¹⁶J. C. Idrobo, S. Ögüt, K. Nemeth, J. Jellinek, and R. Ferrando, *Phys. Rev. B* **75**, 233411 (2007).
¹⁷G. Kresse and J. Hafner, *Phys. Rev. B* **47**, 558 (1993); G. Kresse and J. Furthmüller, *ibid.* **54**, 11169 (1996); P. E. Blöchl, *ibid.* **50**, 17953 (1994).